

Power and Pressure Fluctuations in Elastic Turbulence over a Wide Range of Polymer Concentrations

Yonggun Jun and Victor Steinberg

Department of Physics of Complex Systems, Weizmann Institute of Science, Rehovot, 76100 Israel

(Received 16 October 2008; published 24 March 2009)

Injected power P and pressure p fluctuations in a swirling flow of polymer solutions in a wide range of polymer concentrations c in elastic turbulence regime show non-Gaussian statistics that strongly resemble statistical behavior of P and p in hydrodynamic turbulence. Together with this fact, weak dependence of the statistics of rescaled variables on c may suggest that there are universal mechanisms determining the intermittent statistics of P and p . We also show that the study of the statistics of p provides a way to study statistics of the elastic stresses in elastic turbulence otherwise currently unattainable.

DOI: 10.1103/PhysRevLett.102.124503

PACS numbers: 47.20.Gv, 47.27.-i, 47.50.-d

Many statistical and scaling properties of elastic turbulence in the von Kármán swirling flow between rotating disks were studied in detail as a function of the Weissenberg number, Wi , for a *single* polymer concentration of a polyacrylamide (PAAm) dilute solution [1,2]. The polymer concentration is another important control parameter to vary, since the properties of a polymer solution as well as its flow characteristics drastically depend on it.

Here we present the first systematic studies of the concentration dependence of the properties of elastic turbulence, namely, injected power P and dynamic pressure p fluctuations. Elastic turbulence is a spatially smooth, random in time flow driven entirely by nonlinear elastic stress at Reynolds number $Re < 1$ and at $Wi > 1$. The latter is defined as the ratio of the nonlinear elastic stresses to the linear stress relaxation and quantifies the degree of polymer stretching. The same random in time and spatially smooth flow occurs in high Re hydrodynamic turbulence below the dissipation scale ξ . The polymer molecule being introduced into turbulent flow experiences just small scale velocity fluctuations, since its stretching length remains far below ξ . This means that properties of elastic turbulence and particularly statistics of elastic stresses and polymer stretching are expected to be similar to those in turbulent drag reduction. On the other hand, study of these properties in elastic turbulence is more attainable.

During the last 15 years statistics and correlations of P and p temporal fluctuations in high Re von Kármán swirling flow were studied experimentally and numerically intensively [3–8]. The results of these studies are the following. Statistics of the global, spatially averaged injected power at the constant rotation speed in the confined geometry swirling flow show slight deviation in its probability distribution function (PDF) from Gaussian behavior, mostly due to skewness in the direction of low power consumption, which grows with Re [6–8]. This asymmetry in the PDF occurs due to an excess of low dissipation compared to high dissipation events and shows up in intermittent and drastic power drops in time series over a

wide range of magnitudes. These drops in P strongly correlate with the nonlocal pressure depressions. The time delay between the lowest p and P drops is about the rotation period T_r [7,8]. On the other hand, the PDFs of p fluctuations are strongly non-Gaussian and display an exponential tail toward low pressures that is ascribed to pressure bursts associated with the formation of tubelike vortical structures (filaments) [3–5]. The PDF of time intervals between the drops in time series of p fluctuations reveals an exponential tail at times longer than T_r . This means that the p drops are uncorrelated. At time scales shorter than T_r , the PDF shows an algebraic decay with the exponent of about -1.5 that indicates the strongly correlated events [4]. The time intervals scaled by T_r are independent of Re [4,5]. Thus, the intermittent statistics of P and p fluctuations have the same source, namely, formation and breakdown of the low-pressure filaments with strong vorticity concentration.

In this Letter we present the statistics, scaling, and correlations of P and p fluctuations in elastic turbulence as a function of Wi and in a wide range of polymer concentrations from dilute to over semidilute regimes.

The experiments were conducted in a cylindrical container mounted on a commercial rheometer (AR-1000N from TA Instruments) with the rotating upper disk attached to its shaft. The whole setup was placed into a temperature controlled box at 22.8 ± 0.1 °C. This arrangement allowed precise control (within 0.5%) of the disc angular velocity, Ω , and measurements of the torque and torque fluctuations, or the control of the torque and measurements of Ω . The radii of the upper and the lower plates, separated by $d = 1$ cm, were $R_u = 4.7$ cm and $R_l = 4.9$ cm, respectively. For the swirling flow between the disks, the shear rate can be defined as $\dot{\gamma} = \frac{\Omega \cdot R_u}{d}$ and $Wi = \dot{\gamma} \lambda$, where λ is the longest polymer relaxation time, and Ω is in the range between 0.1 and 2.3 rad/s. A piezoresistive silicon pressure sensor (Honeywell, 40PC001B1A), fully calibrated and compensated with sensitivity of 0.3 mV/Pa and active diameter of 2.8 mm was used for pressure measurements. It

was mounted on the sidewall at midheight. As a working fluid, we used a water-saccharose solution of high-molecular-weight PAAm (MW = 18 MDa, from Polysciences) at various concentrations from 100 ppm till 3000 ppm. As a solvent, water with 66% of saccharose and the addition of 1% NaCl and 250 ppm NaN_3 , that provided solvent viscosity $\eta_{\text{solv}} = 91$ cP, was used for solutions with $c \leq 900$ ppm. For solutions with higher polymer concentrations, sugar was added into a 1% polymer concentration master solution to reach required polymer concentrations. The stress relaxation measurements to obtain λ were conducted in a cone-and-plate geometry on AR1000N rheometer [9].

A wide range of polymer concentrations, from a dilute region $c < c^*$ with $c = 100$ ppm, through a semidilute unentangled region $c^* < c < c_e$ with c between 300 and 900 ppm, till a semidilute entangled region $c > c_e$ with c between 1600 and 3000 ppm, was used in the experiment. Here c^* and c_e are the overlapping concentration and the entanglement concentration in the semidilute regime, respectively [10]. Different concentration regions were identified according to the different scaling of the measured λ versus c (see for details Ref. [11]). The properties of the solutions relevant to the experiment are presented in Table I.

The data on P and p fluctuations were collected simultaneously. For each run for specific values of c and Wi , the PDF for each variable was based on about 2×10^4 data points, except a special long run for $c = 300$ ppm at the highest value of Wi , where about 10^5 data points were collected. At $c = 100$ ppm, the collapse of PDFs at different Wi in elastic turbulence is observed (data are not shown), similar to what has already been reported for 80 ppm [2]. As pointed out in Ref. [2], deviation from Gaussian statistics for P in elastic turbulence occurred due to physical reasons distinctly different from those in high Re turbulence. Figure 1(a) and 1(b) presents PDFs of $\delta P/P^{\text{rms}}$ and $\delta p/p^{\text{rms}}$ fluctuations for c from 100 till 3000 ppm at the highest attained Wi , where $\delta P = P - \bar{P}$ and $\delta p = p - \bar{p}$, and P^{rms} and p^{rms} are the rms values. One notices that the PDFs for both variables are skewed toward the negative values, weaker for $\delta P/P^{\text{rms}}$ and stronger for $\delta p/p^{\text{rms}}$, and exhibit exponential tails. The former feature is quantified in Fig. 1(c).

Skewness, S , and flatness, F , for both the P and p PDFs are practically independent of c up to 900 ppm, and the

TABLE I. Properties of polymer solutions and flow characteristics are: η is the solution viscosity, Wi_c is the threshold value of the elastic instability.

c (ppm)	100	300	500	700	900	1600	2300	3000
η (cP)	146.5	214.1	327.3	424.6	477.7	550.6	643.1	1162.1
λ (s)	10	14	20	24	28	38	44.9	52
Wi_c	50	32	32	32	32	57	57	57

PDFs for $\delta p/p^{\text{rms}}$ deviate much stronger from the Gaussian distribution than for $\delta P/P^{\text{rms}}$. At $c > 900$ ppm the PDFs of both variables become closer to each other. Figure 1(d) shows p^{rms}/\bar{p} versus Wi/Wi_c in the whole range of the polymer concentrations studied. The data are consistent with $p^{\text{rms}}/\bar{p} \propto (\text{Wi}/\text{Wi}_c)^3$, where \bar{p} is the constant. Normalized power fluctuations P^{rms}/\bar{P} are practically independent of Wi/Wi_c in elastic turbulence for all c . The normalized average injected power \bar{P}/P^{lam} shows the same exponent in the scaling dependence against Wi/Wi_c for $c \leq 900$ ppm as reported in Ref. [2], namely $\bar{P}/P^{\text{lam}} \propto (\text{Wi}/\text{Wi}_c)^{0.49 \pm 0.05}$, while it increases up to 0.8 for higher c from 1600 up to 3000 ppm.

Power-law decays in the power spectra of P and p fluctuations in the frequency domain (normalized by the vortex rotation frequency, f_v , which is 0.1 Hz at the most at the highest Wi) for $c \leq 900$ ppm with the exponents -4 and -3 , respectively, are shown in Fig. 2. One notices smeared peaks in the spectra for both P and p at $f/f_v \approx 1$ and the flat spectra at $f < f_v$. Sharp decay in the P spectra at $f/f_v > 1$, which is also observed at c up to 3000 ppm with the same exponent -4 , and similar decay in the p spectra with the exponent -3 , probably, reflects the sharp reduction in contribution of the higher order modes in the velocity and velocity gradient spectra [1] and so in elastic stresses. At higher c up to 3000 ppm, the power decay for the p spectra has the exponent -2.3 . Strong correlation between P and p fluctuations for all concentrations is characterized by cross-correlation functions for several c in the inset in Fig. 2. Correlation times of both P and p fluctuations are of the order of the rotation period $T_r = 2\pi/\Omega$ for all Wi .

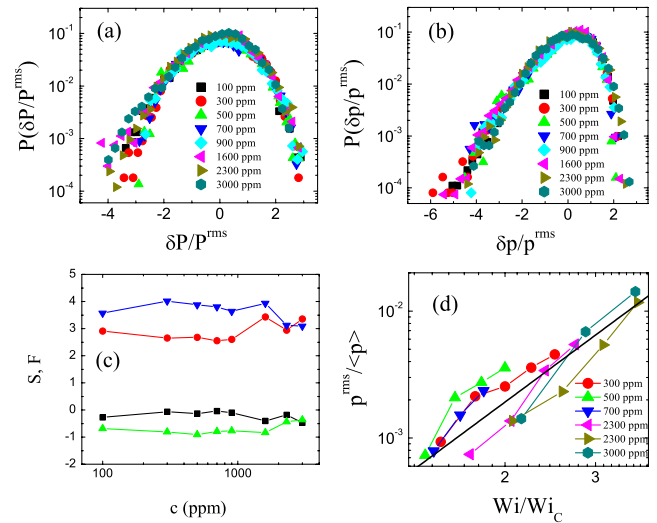


FIG. 1 (color online). (a) PDFs of $\delta P/P^{\text{rms}}$ at different c ; (b) PDFs of $\delta p/p^{\text{rms}}$ at different c ; (c) Skewness, S (squares: power, triangle-up: pressure), and flatness, F (circles: power, triangle-down: pressure), of PDFs as a function of c ; (d) The normalized pressure fluctuations vs Wi/Wi_c for different c . Solid line is a guide for the eye with a slope 3.

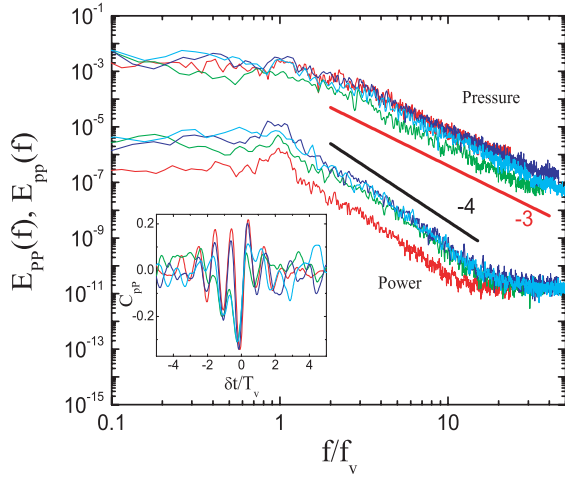


FIG. 2 (color online). Power spectra of P and p fluctuations for $c \leq 900$ ppm. Inset: Cross correlation functions between P and p for several c .

Another way to characterize statistics of a random occurrence of strong drops in the P and p time series is to study: (i) the average duration (width) of the power δt_p and pressure δt_P drops; (ii) the time intervals between the drops in power Δt_p and pressure Δt_P time series; and (iii) the PDFs of Δt_p and Δt_P . Only those drops are selected that are deeper than twice of rms values. One can clearly see in the insets in Figs. 3(a) and 3(b) that both times scaled by T_r for P and p are independent of Wi for 100 ppm solution and have fixed values: for P about 20

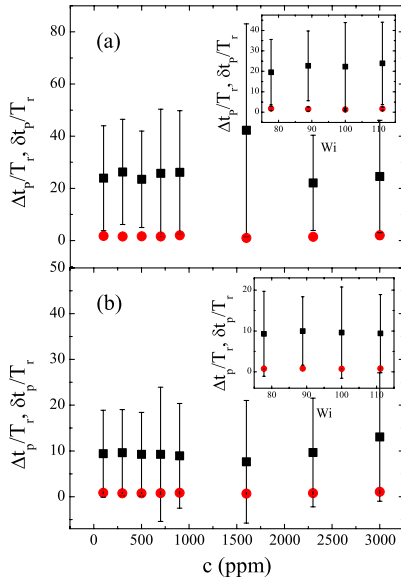


FIG. 3 (color online). (a) Scaled time intervals (squares) and widths (circles) of P drops vs c for the highest Wi ; Inset: The same vs Wi for 100 ppm solution; (b) Scaled time intervals and widths of p drops vs c for the highest Wi ; Inset: The same vs Wi for 100 ppm solution.

and 1.5, and for p about 10 and 0.8, respectively. The main plots in Figs. 3(a) and 3(b) show independence of the same scaled times at maximal values of Wi on c . The reason for about twice differences in the both time intervals for P and p is smaller bursts in P than in p : a significant part of the P drops remains below $2P^{rms}$. Much larger statistics of P and p taken for 300 ppm solution allow us to reproduce PDFs of the time intervals $\Delta t_p/T_r$ and $\Delta t_P/T_r$ (each one based on about 600 points) that are displayed in Fig. 4. The PDF of $\Delta t_p/T_r$ shows the exponential tail $\exp(-\Delta t_p/\tau)$ with the characteristic decay time $\tau \approx 30T_r$ (lower inset), while the PDF of $\Delta t_P/T_r$ has $\exp(-\Delta t_P/\tau)$ decay with $\tau \approx 12T_r$ on the longer times (main plot), and the algebraic decay with the exponent -0.8 on the shorter times (upper inset). The crossover time between two decay laws is of the order of $\Delta t_p^{cross}/T_r \approx 10$. Thus, at larger times the drops in both P and p are statistically independent, while at shorter times the p drops are strongly correlated. The PDFs of the spike widths for both P and p also exhibit exponential tails (data are not shown).

To further characterize the intermittent properties of a stochastic stationary signal one computes the structure functions of the increments of P and p fluctuations defined as $S_n(t) \equiv \langle |Q(t+t_0) - Q(t_0)|^n \rangle_{t_0}$, where $Q(t)$ is either P or p , and looks for a scaling with t in the form $S_n(t) = t^{\zeta_n}$. The dependence of ζ_n/ζ_2 on the order of the structure function, n , up to $n = 6$ is shown in Fig. 5 for both P and p in a wide range of c from 500 up to 3000 ppm. However, if the power spectrum is steep $E(f) \sim f^{-m}$ with $m > 3$ like for both P and p , then $S_2(t) \sim t^2$ for all m and the intermittency is suppressed. Then the structure functions $\tilde{S}_n(t) \equiv \langle |\Delta Q(t)|^n \rangle$ of the second order differences $\Delta Q \equiv Q(t+t_0) - 2Q(t_0) + Q(t_0-t)$ give clearer test for the intermittency [12]. The corresponding exponents $\tilde{\zeta}_n/\tilde{\zeta}_2$ versus n are also shown in Fig. 5. First, $\tilde{\zeta}_n/\tilde{\zeta}_2$ shows

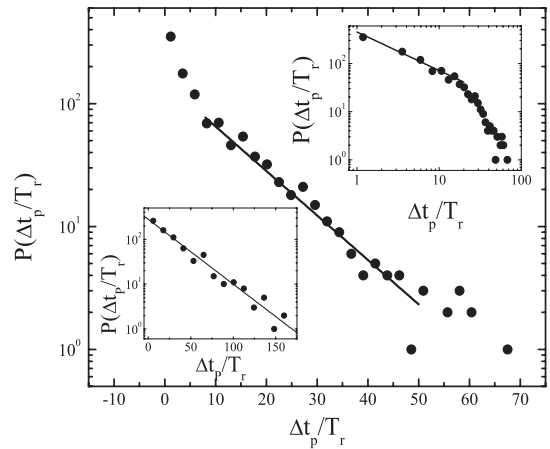


FIG. 4. PDF of $\Delta t_p/T_r$ for p at 300 ppm. Lower inset: The same for P . The solid lines are exponential fits. Upper inset: PDF of $\Delta t_p/T_r$ for p in log-log coordinates; the solid line is the fit at short times with slope -0.8 .

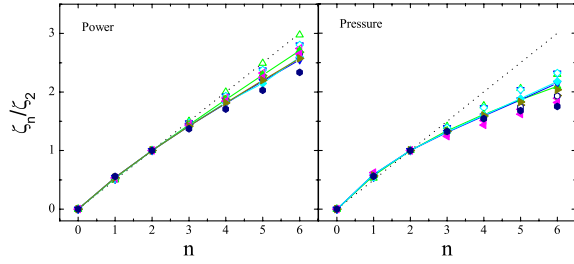


FIG. 5 (color online). ζ_n/ζ_2 vs n for both P and p fluctuations for different c . Symbols open— ζ_n/ζ_2 , full— $\tilde{\zeta}_n/\tilde{\zeta}_2$. All symbols as in Fig. 1.

stronger deviation from linear behavior than ζ_n/ζ_2 for both P and p fluctuations, and second, the larger the concentration, the stronger the deviation from the linear dependence.

In spite of the apparent similarity in statistical behavior of P and p fluctuations in high Re and elastic turbulence, the underlying mechanisms in the both cases are entirely different. An excess of the elastic stress, accumulated near the upper disk due to a constant momentum flux, is intermittently injected into the bulk that results in reduction of the injected power measured on the disk [2]. It may become an origin of the observed exponential tail and the skewness of the PDF towards the small values of $\delta P/P^{\text{rms}}$. Since P and p fluctuations are strongly correlated, the stress excursions into the bulk should cause the p drops resulting in strongly intermittent statistics.

Another source of the intermittent statistics of p can be associated with the elastic stress field reorganization in the bulk. As suggested [2], the elastic stress field is stretched and folded by the flow that leads to non-Gaussian statistics. Since the stress perturbations occur in a whole volume, p fluctuations are nonlocal. The stress dynamics is also reflected in the algebraic decay of the power spectra for both P and p fluctuations.

The important relation between p and elastic stress tensor σ_{ik} is obtained, in the approximation $\text{Re} \ll 1$ and $\text{Wi} \gg 1$ relevant to elastic turbulence, from the equations, analogous to equations for viscosity-dominated magneto-hydrodynamics (MHD), which describe the dynamics of the elastic stress field [13]:

$$\nabla_p = \rho(\mathbf{B} \cdot \nabla)\mathbf{B} + \eta \nabla^2 \mathbf{V}, \quad \nabla \cdot \mathbf{V} = 0, \quad (1)$$

$$\partial_t \mathbf{B} + (\mathbf{V} \cdot \nabla)\mathbf{B} = (\mathbf{B} \cdot \nabla)\mathbf{V} - \mathbf{B}/\lambda, \quad \nabla \cdot \mathbf{B} = 0. \quad (2)$$

Here the vector \mathbf{B} is an analog of the magnetic field in MHD and defined as $\sigma_{ik} = B_i B_k$. The uniaxial presentation is justified, if thermal fluctuations and polymer non-linearity are neglected [13]. After straightforward transformations of Eqs. (1) and (2) one gets

$$\Delta p/\rho = \partial^2 \sigma_{ij}/\partial x_i \partial x_j. \quad (3)$$

This equation is analogous to one that follows from Navier-Stokes equation and used in high Re turbulence. There p is related to velocity gradients via the Poisson equation and so their statistics are related [3,5,14]. Similarly, according to Eq. (3), the intermittent statistics of the elastic stresses in elastic turbulence is the source of the intermittency in the p statistics observed in the experiment. So one suggests that the PDF of p provides a way to study statistics of the elastic stresses in elastic turbulence that are otherwise currently unattainable.

To summarize, we show that a direct relation exists between p and $\sigma_{i,j}$ and so between their statistical properties. It is suggested that the spatial and temporal dynamics of the stress field in the bulk and boundary layer in elastic turbulence results in the intermittent statistics of P and p . Apparent striking similarity in statistical properties of P and p fluctuations in high Re and elastic turbulence and independence of their statistics on c and Wi , despite of different underlying physical mechanisms, suggests universality in statistical properties of P and p in a wide class of nonequilibrium hydrodynamic systems.

We thank M. Chertkov for helpful remarks. This work is supported by grants from Israel Science Foundation, Israeli Ministry of Science, Culture & Sport for Russian-Israeli Cooperation, Lower Saxony Ministry of Science and Culture Cooperation Grant, and by the Minerva Center for Nonlinear Physics of Complex Systems.

-
- [1] A. Groisman and V. Steinberg, *Nature (London)* **405**, 53 (2000); *New J. Phys.* **6**, 29 (2004).
 - [2] T. Burghlea, E. Segre, and V. Steinberg, *Phys. Rev. Lett.* **96**, 214502 (2006); *Phys. Fluids* **19**, 053104 (2007).
 - [3] S. Fauve, C. Laroche, and B. Castaing, *J. Phys. II (France)* **3**, 271 (1993).
 - [4] P. Abry, S. Fauve, P. Flandrin, and C. Laroche, *J. Phys. II (France)* **4**, 725 (1994).
 - [5] O. Cadot, S. Douady, and Y. Couder, *Phys. Fluids* **7**, 630 (1995).
 - [6] R. Labbe, J.-F. Pinton, and S. Fauve, *J. Phys. II (France)* **6**, 1099 (1996).
 - [7] J.-F. Pinton, P. C. Holdsworth, and R. Labbe, *Phys. Rev. E* **60**, R2452 (1999).
 - [8] J. H. Tison and O. Cadot, *Phys. Fluids* **15**, 625 (2003).
 - [9] Y. Liu, Y. Jun, and V. Steinberg, *Macromolecules* **40**, 2172 (2007).
 - [10] M. Doi and S.F. Edwards, *The Theory of Polymer Dynamics* (Clarendon Press, Oxford, 1986).
 - [11] Y. Liu, Y. Jun, and V. Steinberg, *J. Rheol. (N.Y.)* (to be published).
 - [12] E. Falcon, S. Fauve, and C. Laroche, *Phys. Rev. Lett.* **98**, 154501 (2007).
 - [13] A. Fouxon and V. Lebedev, *Phys. Fluids* **15**, 2060 (2003).
 - [14] L.D. Landau and E.M. Lifschitz, *Fluid Mechanics*, (Pergamon Press, Oxford, 1987).